Characteristics of CO2 Absorption into Aqueous Ammonia

You Jeong Kim[a]; Jong Kyun You[a]; Won Hi Hong[a]; Kwang Bok Yi[b]; Chang Hyun Ko[b]; Jong-Nam Kim[b]
[a] Department of Chemical and Biomolecular Engineering, Korea Advanced Institute of Science and Technology, Daejeon, Republic of Korea [b] Chemical Process Research Center, Korea Institute of Energy Research, Daejeon, Republic of Korea

PLEASE SCROLL DOWN FOR ARTICLE

Characteristics of CO_2 Absorption into Aqueous Ammonia

**You Jeong Kim,[1] Jong Kyun You,[1] Won Hi Hong,[1]
Kwang Bok Yi,[2] Chang Hyun Ko,[2] and Jong-Nam Kim[2]**

[1]Department of Chemical and Biomolecular Engineering, Korea
Advanced Institute of Science and Technology, Daejeon,
Republic of Korea
[2]Chemical Process Research Center, Korea Institute of Energy Research,
Daejeon, Republic of Korea

Abstract: Aqueous ammonia was investigated as a new absorbent of the chemical absorption process for CO_2 capture from combustion flue gas. The effects of the temperature and concentration of aqueous ammonia on CO_2 absorption in a semi-batch reactor were studied by interpreting breakthrough curves. Raman spectroscopy analysis of CO_2 loaded aqueous ammonia provided concentration changes of bicarbonate, carbonate, and carbamate as well as CO_2 sorption capacity at given time during the absorption with 13 wt% aqueous ammonia at 25°C. It was observed that carbamate formation was dominating at the early stage of absorption. Then, the bicarbonate formation took over the domination at the later stage while the carbonate remained unchanged.

Keywords: Aqueous ammonia, absorption, CO_2, bicarbonate, carbonate, carbamate, Raman

INTRODUCTION

Much research has been performed for CO$_2$ capture from various industrial gas streams in order to reduce the contribution of CO$_2$ to global warming. Although being the most effective for CO$_2$ capture, the chemical absorption process based on amines such as monoethanolamine (MEA) is still too expensive to apply for large CO$_2$ sources like power plants. In addition, it has been well known that the amine process has inherent problems such as absorbent degradation by acidic compounds and oxygen in gas stream, high energy consumption, and equipment corrosion (1). Recently, aqueous ammonia has been suggested as a new absorbent which can avoid the above problems. The aqueous ammonia has larger capacity of CO$_2$ compared to the amine solution, low regeneration energy required, low material cost, and potential ability to capture acidic gases in flue gas (2–6). However, there are only few research reports available in the use of aqueous ammonia for CO$_2$ capture. Thus, the characteristics of CO$_2$ absorption into ammonia have not been fully investigated and it requires further in-depth study. In this work, the effects of temperature and concentration of aqueous ammonia on CO$_2$ absorption capacity were investigated using a semi-batch reactor, and the concentration changes of carbon containing species during the absorption were also studied using Raman spectroscopy. The bubbling enhanced feature of the reactor reduced the gas-liquid mass transfer resistance remarkably. Hence, the CO$_2$ gas could be absorbed more rapidly into aqueous ammonia. The extremely sharp breakthrough curves were obtained by the reactor and the breakthrough point at given condition was used for interpreting characteristics of CO$_2$ absorption into aqueous ammonia.

Raman Analysis for CO$_2$ Absorbed Aqueous Ammonia

CO$_2$ is absorbed into aqueous ammonia with following main reactions;

$$NH_3 + H_2O \longleftrightarrow NH_4^+ + OH^- \tag{1}$$

$$CO_2 + H_2O \longleftrightarrow HCO_3^- + H^+ \tag{2}$$

$$HCO_3^- \longleftrightarrow CO_3^{2-} + H^+ \tag{3}$$

$$NH_3 + HCO_3^- \longleftrightarrow NH_2COO^- + H_2O \tag{4}$$

$$H_2O \longleftrightarrow H^+ + OH^- \tag{5}$$
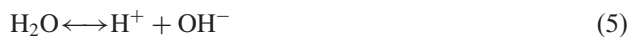
Beside the reactions above, the precipitation reactions of ammonium bicarbonate (NH$_4$HCO$_3$), ammonium carbamate (NH$_2$COONH$_4$), and ammonium carbonate ((NH$_4$)$_2$CO$_3$) may occur depending on operating conditions. In order to understand the absorption mechanism of CO$_2$ into aqueous ammonia, it is needed to analyze the CO$_2$ absorbed solution quantitatively. The established methods like total alkalinity titrimetric method (5) can determine only the

amount of carbonate, bicarbonate, and hydroxide quantitatively. Also it might have some errors caused by neglecting the amount of ammonium carbamate. During CO_2 absorption into aqueous ammonia, ammonium carbamate is formed as well as ammonium bicarbonate and ammonium carbonate. According to the equilibrium data, the amount of ammonium carbamate can not be neglected (7). The titration method suggested by Li (8) has been used to measure the CO_2 capacity in absorbent of amine-based systems. However it cannot provide information of the quantitative changes of the carbon containing species—bicarbonate, carbonate, and carbamate.

To measure the concentrations of three carbon containing species at the same time, the Raman spectra analysis was adopted in this work. Wen and Brooker (9) suggested the factor analysis method to calculate the concentration of the aqueous ammonium carbonate solution from Raman spectra in the region between 965 and 1099.5 cm^{-1}. For a Raman band, the relative intensity, I_i, is directly related to the concentration of a particular species through the expression

$$I_i = J_i m_i \tag{6}$$

where J_i called as the molal intensity coefficient of species i, is the molal intensity of species i for the specified peak normalized to an internal intensity standard of 1.0 mol/kg of $ClO_4^-(aq)$, and m_i is the concentration (in mol/kg) of species i. The relative integrated intensity, I_i, is directly proportional to the band area. The use of an internal intensity standard, 935 cm^{-1} band of $ClO_4^-(aq)$, eliminates the effects of variation in refractive, such as the intensity of the source, sample cell properties, scattering geometry, and instrument sensitivity. Table 1 shows the frequencies and the values of J_i at 25°C.

EXPERIMENTS

CO_2 Absorption into Aqueous Ammonia

The amount of absorbed CO_2 in aqueous ammonia was measured with varying absorption temperature and ammonia concentration. The detailed

Table 1. The frequencies and the values of the molar intensity coefficient at 25°C[a]

Component	Frequency (cm^{-1})	J_i (kg/mol) at 25°C
Bicarbonate, $HCO_3^-(aq)$	1017	0.1990 ± 0.0100
Carbamate., $NH_2COO^-(aq)$	1034	0.402 ± 0.040
Carbonate, $CO_3^{2-}(aq)$	1065	0.3395 ± 0.0170

[a]Data from (9).

experimental procedure is described as follows: The schematic diagram of the absorption experiment to investigate the CO$_2$ absorption characteristics of aqueous ammonia in a semi-batch reactor is shown in Fig. 1. The simulated flue gas consists of 12.81 vol% CO$_2$ and balanced N$_2$. The mixed gas was supplied by compressed gas cylinders, and entered the bottom of reactor at room temperature. The gas flow rate was fixed at 120 SCCM by a mass flow controller (Brooks, 5850E). The pressure was near atmospheric, and measured by a digital pressure sensor. The reactor was a 120 ml glass container whose inner diameter was 1.5 cm, and filled with 70 ml aqueous ammonia. In order to ensure fine distribution of the gas into the liquid, a sintered glass plate (2 μm pore) was placed at the bottom of the reactor. The temperature of the reactant was controlled by the water jacket installed outside of the reactor. The temperature of the reactor was monitored with a thermocouple inside the reactor. The top of reactor was connected to the total reflux condenser whose temperature was set to $-4°C$ to condense the vapor escaping from the reactor. The condensed vapor was continuously drained back to the reactor. The ammonia emission from the

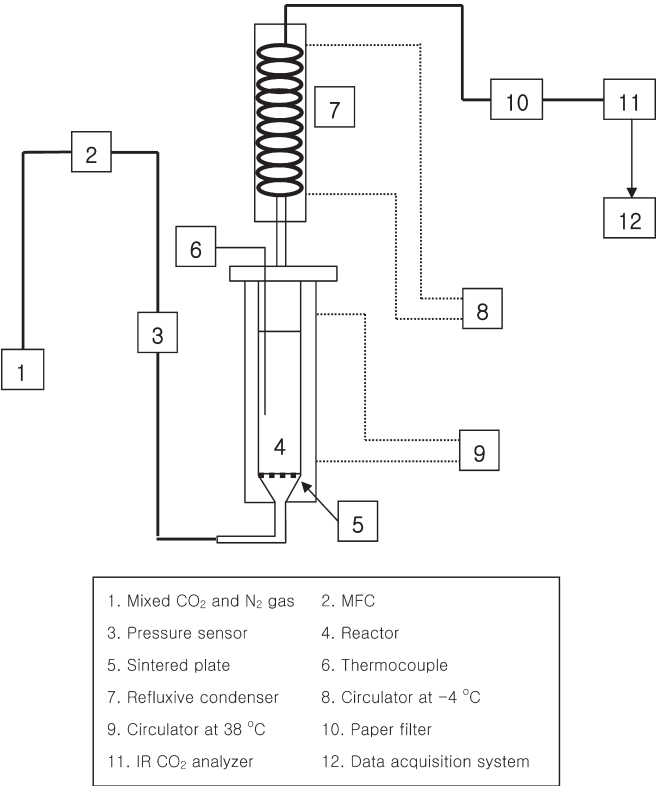|	
1. Mixed CO$_2$ and N$_2$ gas	2. MFC
3. Pressure sensor	4. Reactor
5. Sintered plate	6. Thermocouple
7. Refluxive condenser	8. Circulator at -4 °C
9. Circulator at 38 °C	10. Paper filter
11. IR CO$_2$ analyzer	12. Data acquisition system

Figure 1. Schematic diagram of a semi-batch reactor having bubbling enhanced feature.

reflux condenser was measured by ammonia gas detection tube (RAE SYSTEMS, 1–15%) by every hour. The concentration of ammonia in vent gas was less than 1% during CO_2 absorption. After 7 hour absorption, the aqueous ammonia concentration was reduced from 13 to 12.5 wt%. Therefore, it was assumed that the concentration change by the slipped ammonia was not large enough to affect the experimental results.

The CO_2 concentration in the vent gas was continuously monitored with the IR CO_2 analyzer (Signal Instruments, 7000 FM GFC) and plotted with time. CO_2 sorption capacity at given absorption time and conditions was obtained through numerical integration of the plot.

Analysis of the CO_2 Absorbed Aqueous Ammonia

To analyze the CO_2 absorbed aqueous ammonia, the five sets of CO_2 absorption experiments with different absorption time were carried out using 13 wt% aqueous ammonia and 12.81 vol% CO_2 gas.

The reactor temperature was kept constant at 25°C. The mixed CO_2 gas with the flow rate of 120 SCCM was supplied to the reactor for 3, 4, 5, 6, and 7 hours, respectively. Then the 20 g of CO_2 loaded aqueous ammonia was sampled from each set of experiments for analysis. The pH value was measured by a pH meter (AB15 PLUS, Accument) at room temperature. Then, $NaClO_4$ (SIGMA-ALDRICH, reagent grade) was added as an internal intensity standard. Its concentration for all solutions was kept as 0.5170 mol/kg. The samples were analyzed with Raman spectroscopy at room temperature. The scan rate was $500\ cm^{-1}$ per minute, and the total counts were collected for the time interval that corresponded to a $2\ cm^{-1}$ spectral interval. Five spectra for different absorption time were obtained in the region of $850-1100\ cm^{-1}$ with software called OPUS (OPUS 5.5, Bruker Optik GmbH). Subsequent curve resolution was archived with the PeakFit program (PeakFit version 4, Asian software. Inc.). The method resolves the overlapping bands by fitting a composite envelope obtained from Gauss-Lorentz product functions for the species bands to the experimental band envelope. Areas of the component bands were used to calculate the relative integrated molar intensities and concentrations of the carbon containing species. The relative integrated intensities were converted to molal concentration for each carbon containing species through the (Eq. 6).

RESULTS AND DISCUSSION

CO_2 Absorption into Aqueous Ammonia

The sintered plate located at the bottom of the bubbling enhanced reactor improved the CO_2 absorption by great degree. Figure 2 shows the

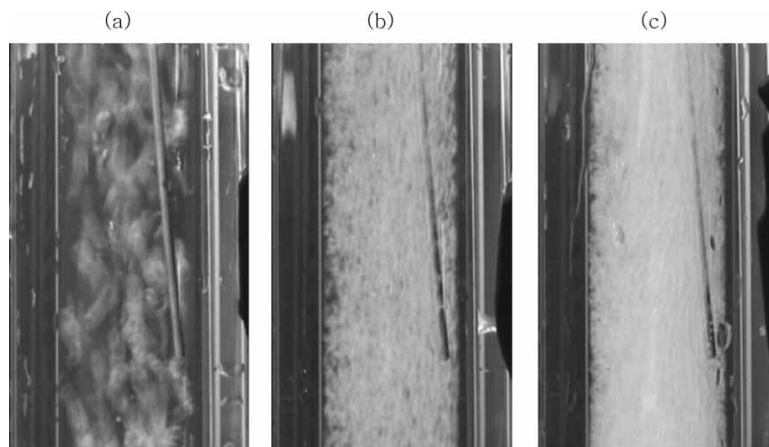(a)   (b)   (c)

Figure 2. Photographs of the bubbling after gas entered the reactor; (a) after 10 seconds; (b) after 15 minutes; (c) after 25 minutes.

photographs of the reactor taken during absorption; (a) after 10 seconds, (b) after 10 minutes, and (c) after 25 minutes. As absorption proceeded, the fine bubbles were formed. These delicate bubbling let the gas-liquid mass transfer resistance reduce remarkably. By using this reactor, the CO$_2$ gas was absorbed into absorber completely until the certain point of absorption time. Afterward, the amount of unreacted CO$_2$ gas increased abruptly. This point was defined as the breakthrough point. As reported in other literature (5), the CO$_2$ concentration in vent gas slowly increases as reaction proceeds in common semi-batch reactor. Therefore, it is quite difficult to define the breakthrough point. However, the reactor configuration used in this study enabled us to pinpoint the breakthrough point because of the sharp breakthrough curve.

Figures 3a and 3b show the breakthrough curves with the different temperatures of reactor and the CO$_2$ loading value changes at the breakthrough point as the temperature increased. The breakthrough point was obtained as an intersection point of X-axis and the steep line showing the increase of the CO$_2$ gas concentration. The CO$_2$ loading value was defined as moles of CO$_2$ per that of ammonia in solution. In general, as the temperature increased, the CO$_2$ absorption capacity decreased. However, there was the optimum temperature for the CO$_2$ absorption into aqueous ammonia and it was near 26°C. This was because at the lower temperature the mass transfer rate decreased enough to offset the increased solubility effect.

The 7, 10, 13, and 17 wt% aqueous ammonia were used to investigate the effect of the concentration at 38°C. The use of aqueous ammonia with concentration of higher than 17 wt% was not attempted because a considerable amount of ammonia loss is expected due to its excessive ammonia vapor
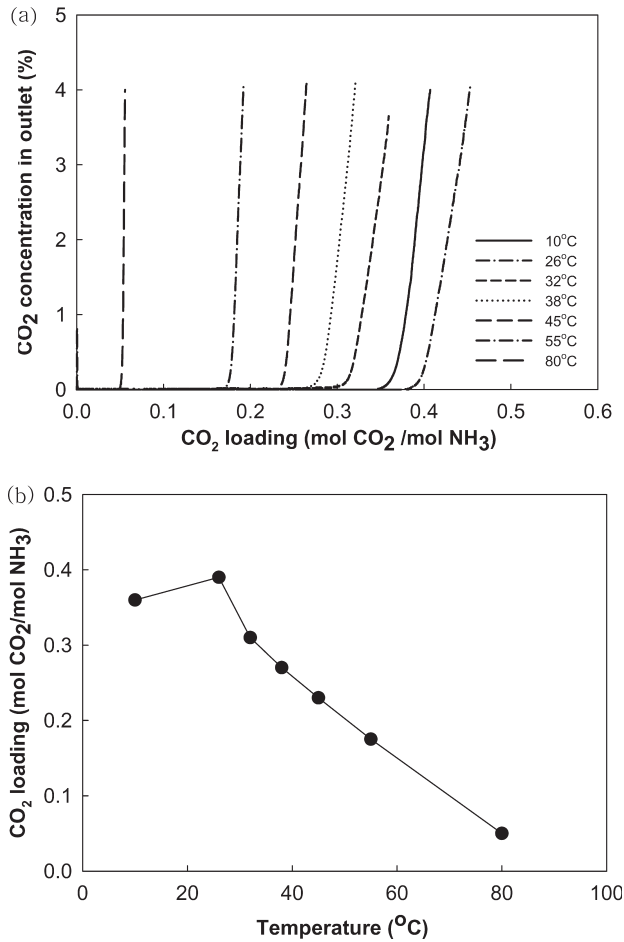
Figure 3. (a) Breakthrough curves and (b) the change of CO_2 loading values at breakthrough point with different aqueous ammonia temperatures.

pressure. Furthermore, the precipitation of ammonium carbamate in the solution is predicted with more than 20 wt% of ammonia concentration at over $30°C$ (7).

Figure 4 shows the change of CO_2 loading and CO_2 sorption capacity with different aqueous ammonia concentration. The CO_2 sorption capacity which represents the absolute amount of absorbed CO_2, was defined as mole of the absorbed CO_2 per kg of aqueous ammonia. Generally, the higher values for both CO_2 loading and CO_2 sorption capacity are favorable for CO_2 absorption process. However, the experimental results in Fig. 4 showed that the CO_2 loading decreased and the CO_2 sorption capacity increased as aqueous ammonia concentration increased. In order
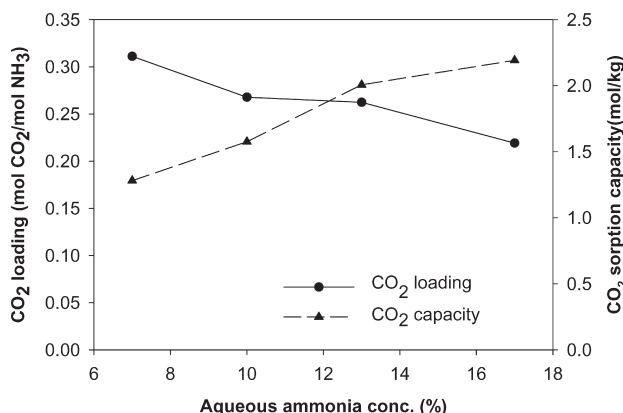
Figure 4. The change of CO$_2$ loading values and CO$_2$ sorption capacity at break-through point with different aqueous ammonia concentrations at 38°C.

to determine a compromising aqueous ammonia concentration, one should find the concentration region that increase CO$_2$ sorption capacity the most and decrease CO$_2$ loading the least. The close examination of the experimental result in Fig. 4 revealed that when the concentration increased from 10 to 13 wt%, the decrement of CO$_2$ loading was smaller than those in other concentration change region. In addition, when aqueous ammonia concentration was higher than 13 wt%, the CO$_2$ loading rapidly decreased but the increment of the sorption capacity was smaller than those in the region below 13 wt%. Thus, considering both the CO$_2$ absorption amount and the effectiveness of ammonia involved in absorption, 13 wt% aqueous ammonia is reasonable choice for the absorption process.

Analysis of CO$_2$ Loaded Aqueous Ammonia

The CO$_2$ absorption experiments were carried out for observing the composition change of CO$_2$ loaded aqueous ammonia. 13 wt% aqueous ammonia at 25°C was used. This condition was suggested as an adequate temperature and ammonia concentration in previous section. In this case, the breakthrough point appeared at 4.9 hours with 12.81 vol% CO$_2$ gas at the flow rate of 120 SCCM. The CO$_2$ loaded aqueous ammonia was analyzed by Raman spectroscopy. The complete band envelope was resolved into the three bands of species with over 99.9% fitting accuracy. An example of the band resolution which can be achieved is shown along with the computer-simulated spectra in Fig. 5(a). It was found that the three bands required by the factor analysis are centered at 1017, 1034, and 1065 cm^{-1}, which are the frequencies assigned for bicarbonate, carbamate, and carbonate, respectively. Figure 5(b) shows the normalized
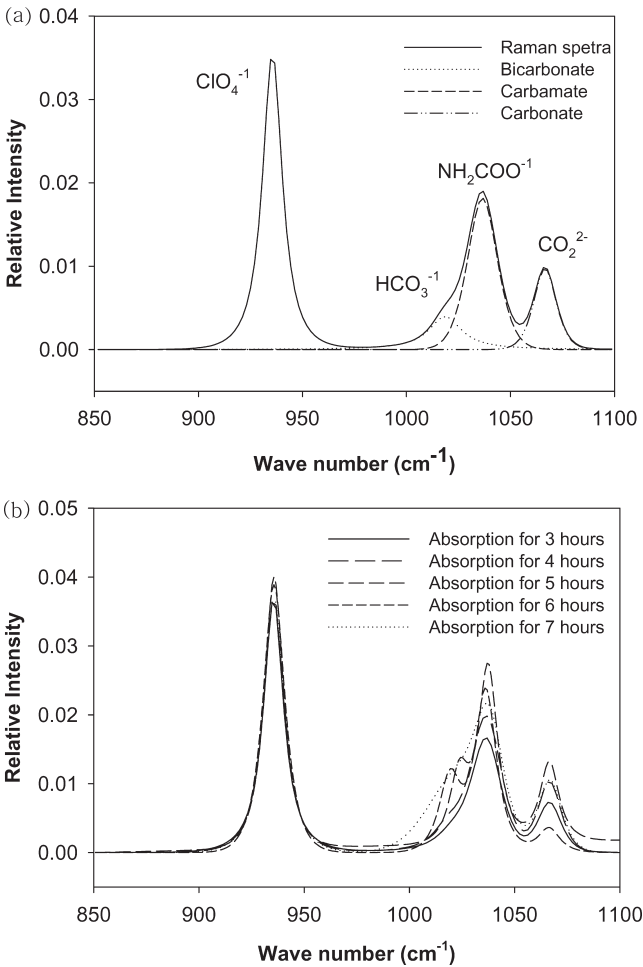
Figure 5. Raman spectra of absorber in the range between 850 and 1100 cm^{-1} during CO_2 absorption into aqueous ammonia; (a) Raman spectrum at room temperature showing resolution of components and computer generated spectrum; (b) Normalized Raman spectrum at room temperature showing the change of concentration during CO_2 absorption for 7 hours.

Raman spectra changes during the CO_2 absorption. As CO_2 was absorbed into aqueous ammonia, the peak area became larger. Figure 6 shows the concentrations changes of carbon containing species as well as CO_2 sorption capacity at 3, 4, 5, 6, and 7 hours absorption. The dashed line represents CO_2 sorption capacity at given time obtained from CO_2 mass balance of the reactor. The pH values at each time were, 10.37, 9.62, 9.31, 9.14, and 9.03, respectively. CO_2 sorption capacity at 7 hours of absorption from Raman analysis was 3.23 mol/kg. At this point, the
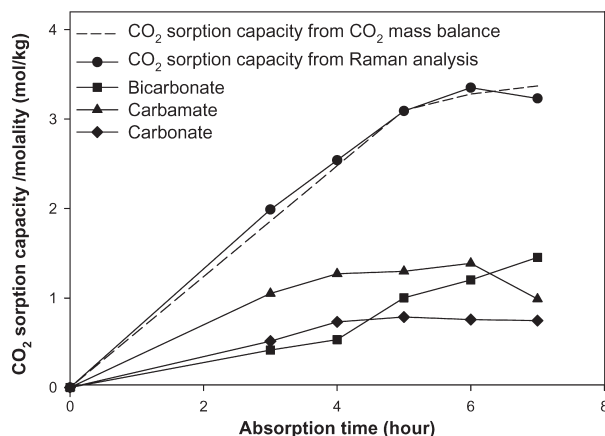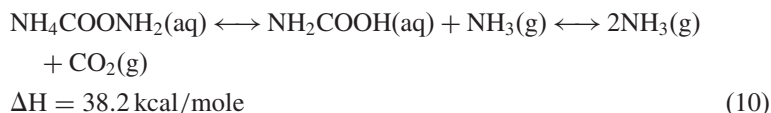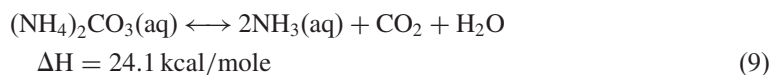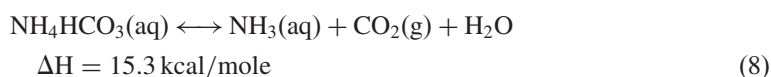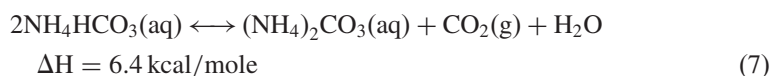
Figure 6. The calculated concentrations of carbon containing species during the absorption and CO$_2$ sorption capacity at given time.

deviation from the concentration calculated from CO$_2$ mass balance, 3.37 mol/kg, was about 4%. For the entire range of absorption time, the deviations were less than 4% except the one at 3 hours of absorption. A bit higher deviation in the early absorption stage might be due to the relatively large error caused by the low concentrations of carbon containing species in the solution. Nevertheless, Raman spectroscopy analysis of the CO$_2$ absorbed aqueous ammonia seemed to provide the quite accurate value of the absorbed CO$_2$ concentration. Hence, it was thought that the concentration changes of other species from Raman analysis also were reliable.

In the early stage of absorption the concentration of carbamate was almost twice higher than those of other carbon containing species, but its concentration increment was getting smaller as the absorption proceeded. After 4 hours of the absorption the bicarbonate concentration increased rapidly, whereas the concentration change of carbonate was very small. After 6 hours pH was 9.14 and the amount of carbamate started to decrease. It seemed that the partial decomposition of carbamate at later stage contributed the continuous further bicarbonate formation. Thus, it is thought that the CO$_2$ absorption in the later stage was mostly contributed by bicarbonate formation. At the point that the bicarbonate concentration started to increase rapidly, its concentration was 0.54 mol/kg, and CO$_2$ sorption capacity was 2.54 mol/kg. Because this bicarbonate formation mostly occurred in the later absorption stage, the regeneration energy required through the bicarbonate decomposition might be the least among various possible routes. In fact, as shown in following equations, the heat of reaction for ammonium bicarbonate decomposition has been known to be the least among the reactions for CO$_2$ desorption (5).

$$2NH_4HCO_3(aq) \longleftrightarrow (NH_4)_2CO_3(aq) + CO_2(g) + H_2O$$
$$\Delta H = 6.4 \, \text{kcal/mole} \tag{7}$$

$$NH_4HCO_3(aq) \longleftrightarrow NH_3(aq) + CO_2(g) + H_2O$$
$$\Delta H = 15.3 \, \text{kcal/mole} \tag{8}$$

$$(NH_4)_2CO_3(aq) \longleftrightarrow 2NH_3(aq) + CO_2 + H_2O$$
$$\Delta H = 24.1 \, \text{kcal/mole} \tag{9}$$

$$NH_4COONH_2(aq) \longleftrightarrow NH_2COOH(aq) + NH_3(g) \longleftrightarrow 2NH_3(g)$$
$$+ CO_2(g)$$
$$\Delta H = 38.2 \, \text{kcal/mole} \tag{10}$$

Therefore, when it comes to continuous CO_2 capture process using aqueous ammonia, it might be beneficial to operate the absorption and the desorption process in the CO_2 loading range that the amount bicarbonate varies the most.

The results of this study could be used in obtaining CO_2 loading value and analyzing the CO_2 loaded aqueous ammonia in further study for the absorption and desorption process using aqueous ammonia.

CONCLUSION

The characteristics of CO_2 absorption into aqueous ammonia in a semi-batch were studied in terms of temperature and ammonia concentration. The reactor used in this study had bubbling enhanced features and extremely sharp breakthrough curves were produced. The appropriate temperature and concentration of aqueous ammonia for the CO_2 absorption process were around $26°C$ and 13 wt%, respectively.

The composition change of CO_2 loaded aqueous ammonia during the absorption and the CO_2 sorption capacity at given time were observed by Raman spectroscopy analysis, which was relatively convenient and accurate. Carbamate formation rate was much faster than other species in the early stage of absorption, and the bicarbonate formation became significant as CO_2 absorption proceeded. In the later stage the CO_2 absorption is thought to be contributed mainly by bicarbonate formation. Furthermore, as previously discussed, ammonium bicarbonate decomposition to ammonium carbonate requires the least energy among the various regeneration reactions. Therefore, it might be beneficial in terms of energy saving to maximize the concentration of ammonium bicarbonate in aqueous ammonia by pre-CO_2-saturation prior to operation of the CO_2 capture process. By this means, the absorption and desorption process using aqueous ammonia is recommended to be operated within the CO_2 loading range where the bicarbonate variation is the most.

REFERENCES

1. Metz, A., Davidson, O., Coninck, H., Loos, M., and Meyer, L. (2005) *IPCC Special Report; Carbon Dioxide Capture and Storage*; International Panel on Climate Change. Cambridge University Press: Cambridge, U.K.
2. Yeh, A.C. and Bai, H. (1999) Comparison of ammonia and monoethanolamine solvents to reduce CO_2 greenhouse gas emissions. *Sci. of Total Environ.*, 228 (2/3): 121.
3. Bai, H. and Yeh, A.C. (1997) Removal of CO_2 Greenhouse gas by ammonia scrubbing. *Ind. Eng. Chem. Res.*, 36 (6): 2490.
4. Diao, Y.F., Zheng, X.Y., He, B.S., Chen, C.H., and Xu, X.C. (2004) Experimental study on capturing CO_2 greenhouse gas by ammonia scrubbing. *Energy Convers. Manage.*, 45: 2283.
5. Yeh, J.T., Resnik, K.P., Rygle, K., and Pennline, H.W. (2005) Semi-batch absorption and regeneration studies for CO_2 capture by aqueous ammonia. *Fuel Processing Tech.*, 86: 1533.
6. Huang, H. and Chang, S.G. (2002) Method to regenerate ammonia for the capture of carbon dioxide. *Energy & Fuels.*, 16: 904.
7. You, J.K., Park, H.S., Hong, W.H., Park, J.K., and Kim, J.N. (2007) Effect of precipitation on operation range of the CO_2 capture process using aqueous ammonia absorbent. *Korean Chem. Eng. Res.*, In Press.
8. Li, M.H. and Chang, B.C. (1994) Solubilities of carbon dioxide in water + monoethanolamine + 2-amino-2-methyl-1-propanol. *J. Chem. Eng. Data.*, 39 (3): 448.
9. Wen, N. and Brooker, M.H. (1995) Ammonia carbonate, ammonia bicarbonate, and ammonium carbamate equilibria: A Raman study. *J. Phys. Chem.*, 99: 359.